

Supplementary Materials for

A Strong Phase Separation Polyurethane for Self-repairing Large-scale Damage

Mengyu Li, Xin Han, Zewen Fan, Hao Chen, Yu Zhang, Lin Zhang, Dan Guo,

Guoxin Xie*

† State Key Laboratory of Tribology, Department of Mechanical Engineering, Tsinghua

University, Beijing 100084, China.

*E-mail: xgx2014@tsinghua.edu.cn

The file includes:

Materials and Methods

Supplementary Text

Figures S1 to S17

Table S1 to S3

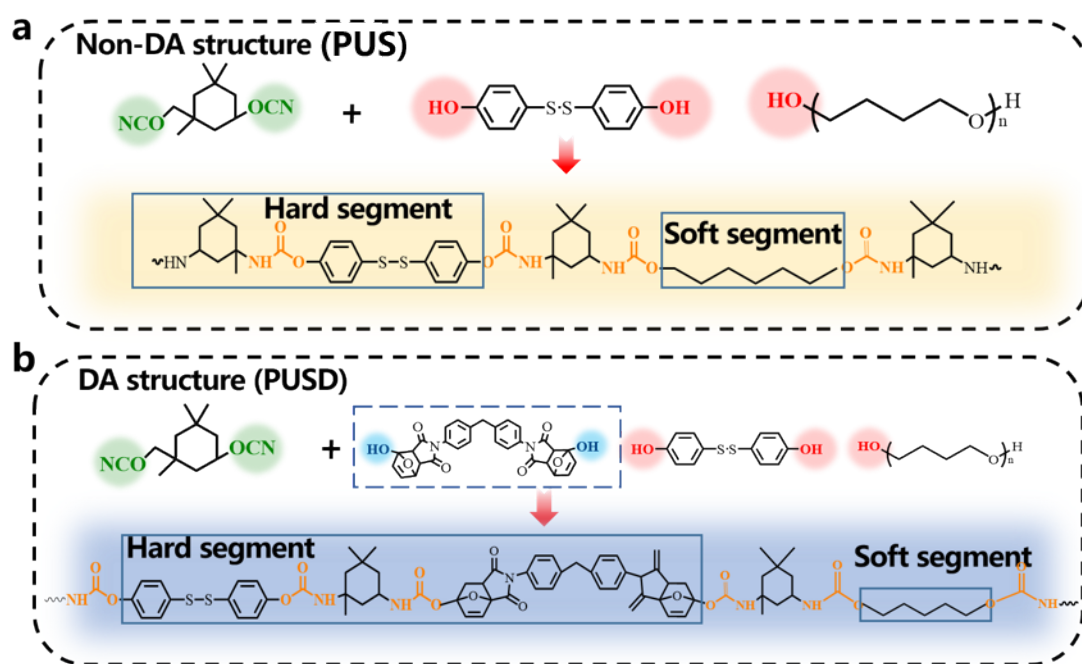


Figure S1. Synthesis paths of the PUS and PUSD samples

On the basis of molecular design, two types of polyurethane have been synthesized. The difference between these two types of polyurethane is the presence or absence of the DA structure.

Table S1. Molar ratios of the DA contents in the polymers

Sample Code	BMI[g]	FA[g]	Molar Content [mol]
PUS	0	0	0
PUSD-1	5.37	2.94	0.015
PUSD-2	7.16	3.92	0.02
PUSD-3	9	5	0.025
PUSD-4	10.75	5.88	0.03

Table S2. Contents of the main materials used for polymer syntheses

Sample Code	PTMEG [g]	BMI [g]	FA [g]	IPDI [g]	DBTDL [mL]	Molar Ratio	Hard
						[PTMEG:BMI:FA]	Segment Content[%]
PUS	12.5	0	0	6.5	0.8	1:0:0	22.7
PUSD-1	12.5	5.37	2.94	6.5	0.8	1:0.37:0.73	30.4
PUSD-2	12.5	7.16	3.92	6.5	0.8	1:0.49:0.98	36.8
PUSD-3	12.5	9	5	6.5	0.8	1:0.61:1.24	42.4
PUSD-4	12.5	10.75	5.88	6.5	0.8	1:0.73:1.46	46.7

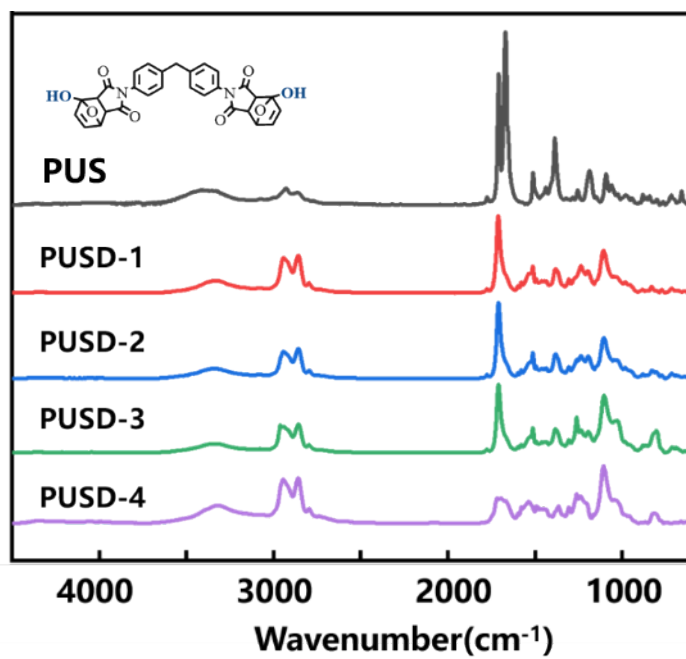


Figure S2. Infrared spectra of the polymers with different DA contents.

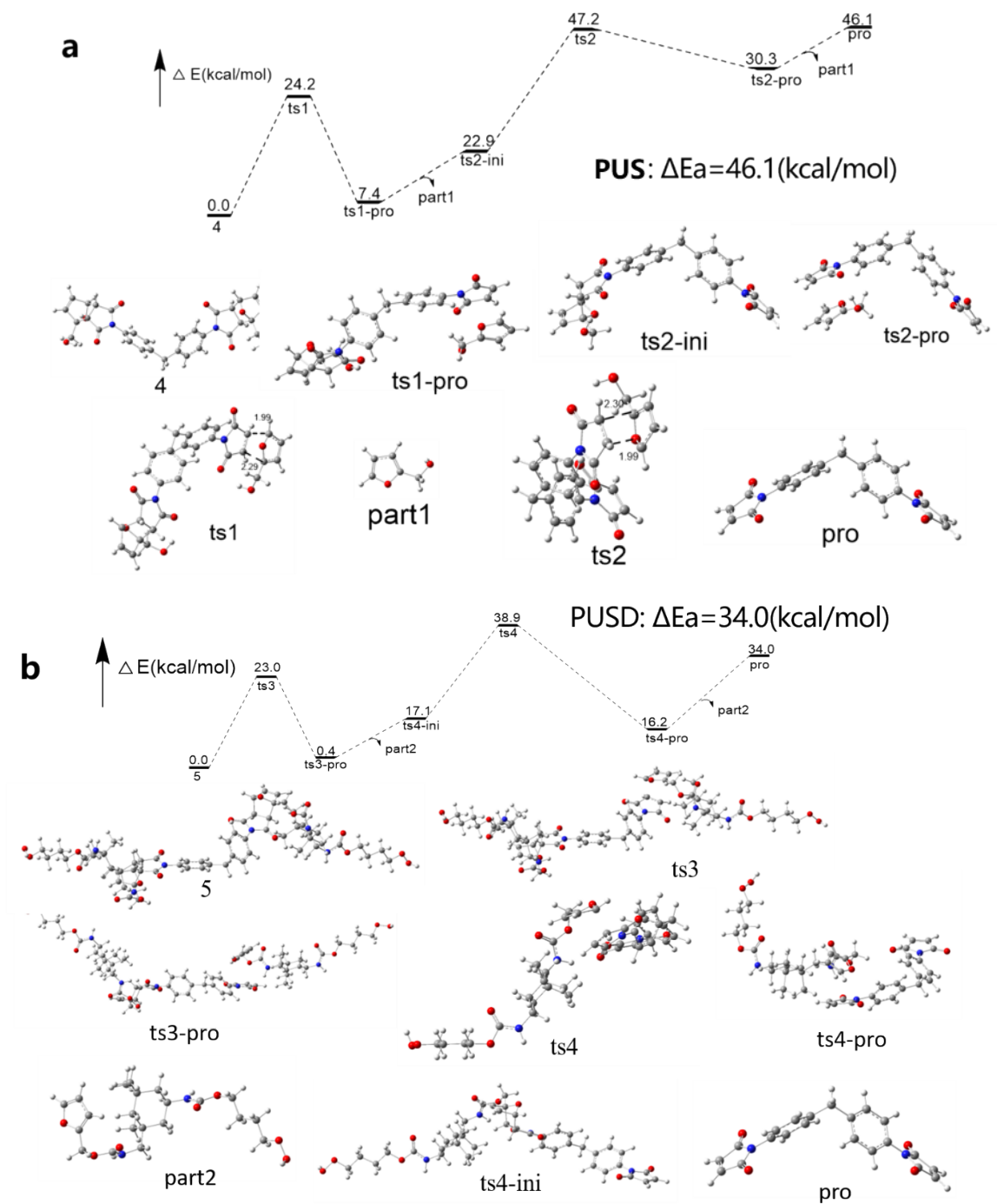


Figure S3. Diagrams of the Gaussian simulations of PUS and PUSD

The Gaussian simulations of the molecular structure show that the activation energy of the chain segment fragmentation reduced to 34.0 kcal/mol after the introduction of the DA structure.

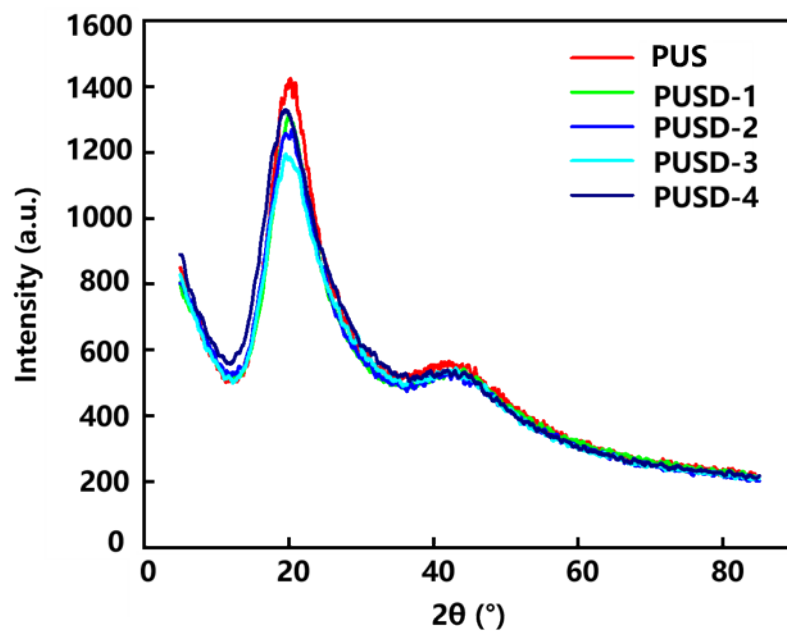


Figure S4. XRD patterns of the polymers with different DA contents

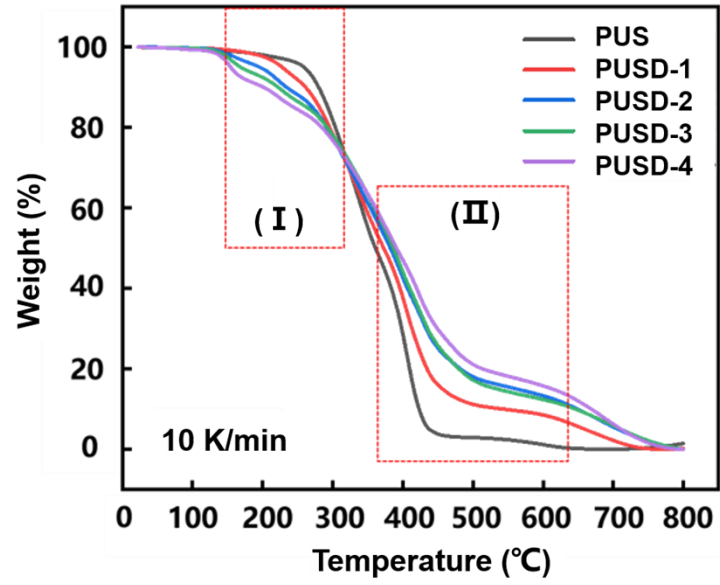


Figure S5. TG curves of the polymers with different DA contents

The molecular asymmetry of the PUSD chain segment was increased after introducing the DA structure. Therefore, the decomposition temperature of PUSD decreased.

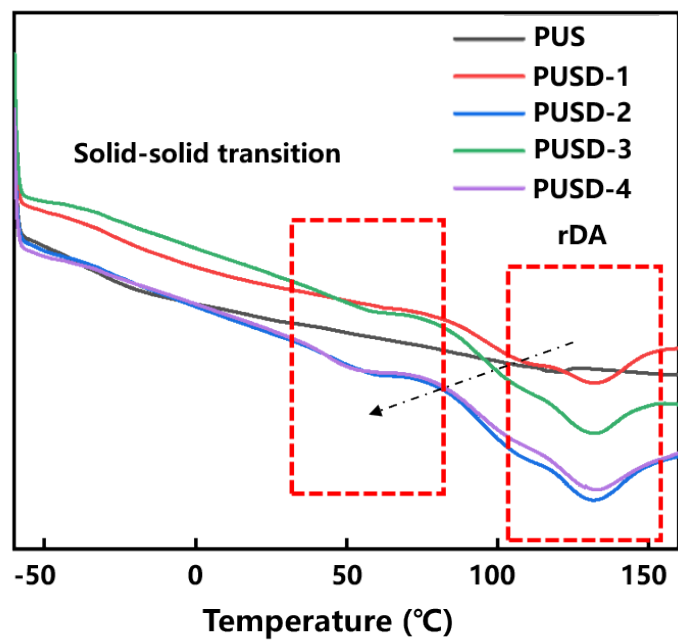


Figure S6. DSC curves of the polymers with different DA contents

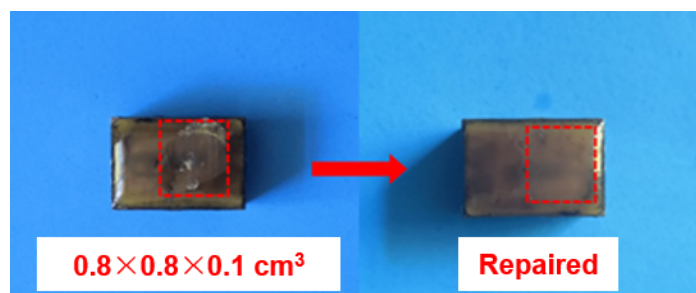


Figure S7. Photos showing the repair effect of the large-scale damage in the PUSD coating.

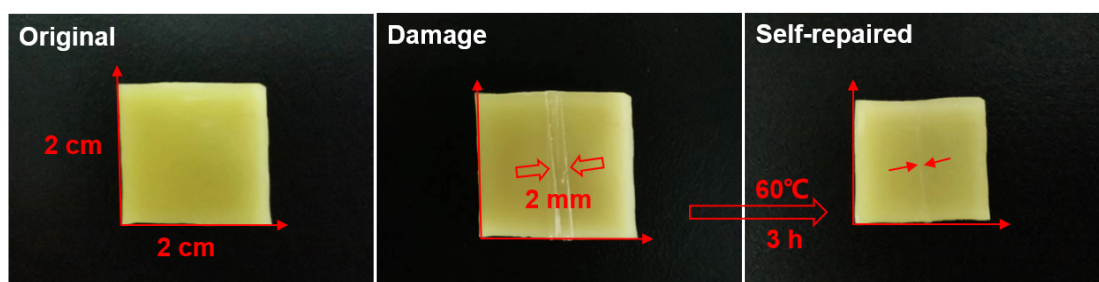


Figure S8. Photos showing the repair effect of the large-scale damage on the surface of the PUSD.

As shown in Figure S7 and Figure S8, the PUSD as the coating was damaged by the ring block tribometer in the area shown in the figure, and the damaged area was $0.8 \text{ cm} \times 0.8 \text{ cm}$, depth was 0.1 cm . It could be repaired, as shown in the Figure S7, and no damage marks were observed. At the same time, a 2-mm-wide crack was created in the block PUSD using a scratcher, and it can be seen that PUSD can achieve a targeted repair of the damage in Figure S8.

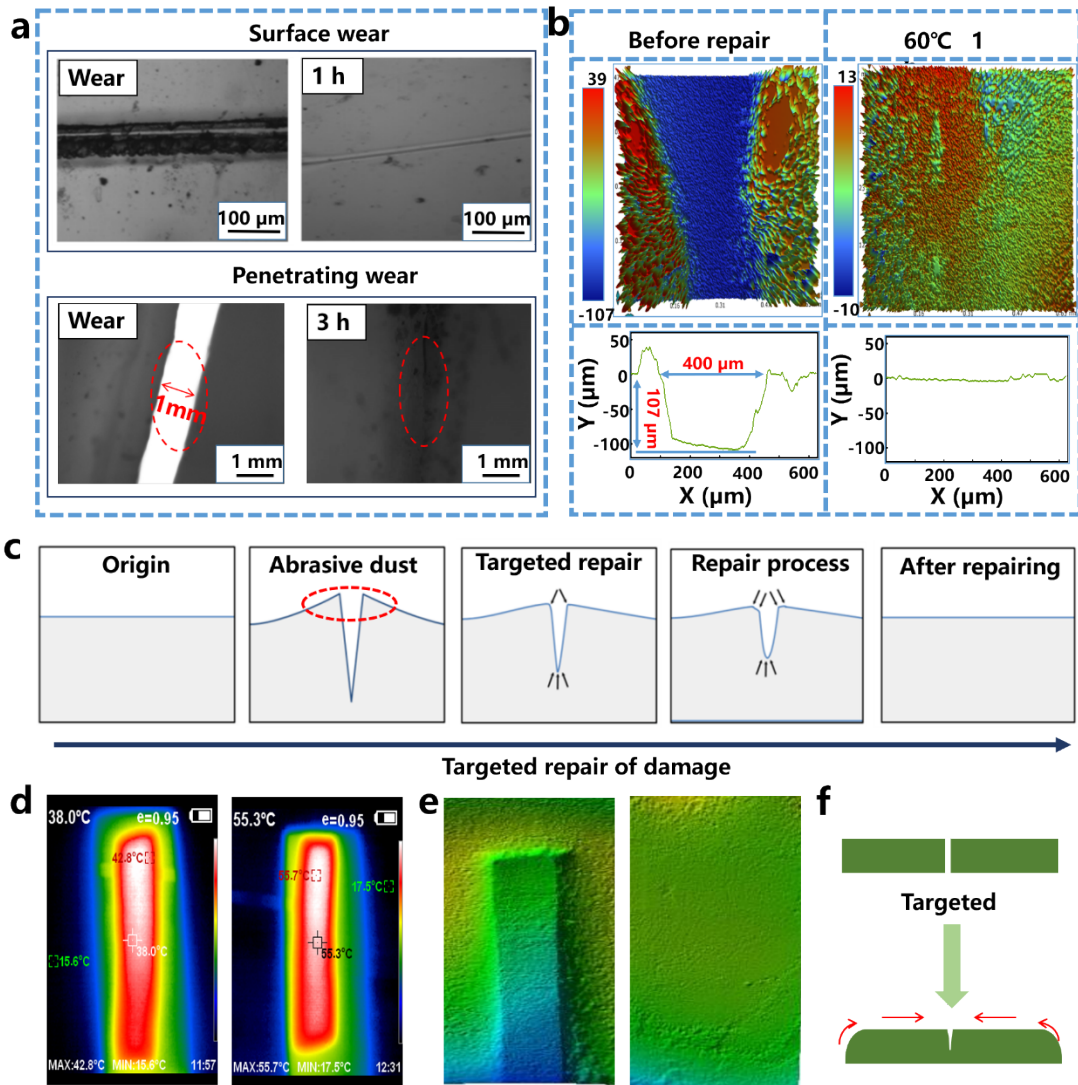


Figure S9. (a) The crack repair experiments at 60 $^{\circ}\text{C}$ for 1 h and the cut-off repair experiments at 60 $^{\circ}\text{C}$ for 3 h of PUSD; (b) The 3D surface topography mapping images of PUSD during the self-repairing process at 60 $^{\circ}\text{C}$ for 1 h and the corresponding depth profiles of PUSD during the self-repairing process at 60 $^{\circ}\text{C}$ for 1 h; (c) Targeted repair process of the damage area of PUSD; (d-f) Infrared thermal imaging photos, 3D topography and self-healing process diagram of the targeted repair of damage area for PUSD.

The repair experiments of large-scale damage were carried out, and the PUSD could achieve not only the targeted repair but also the repairing of larger-scale damage at 60 $^{\circ}\text{C}$.

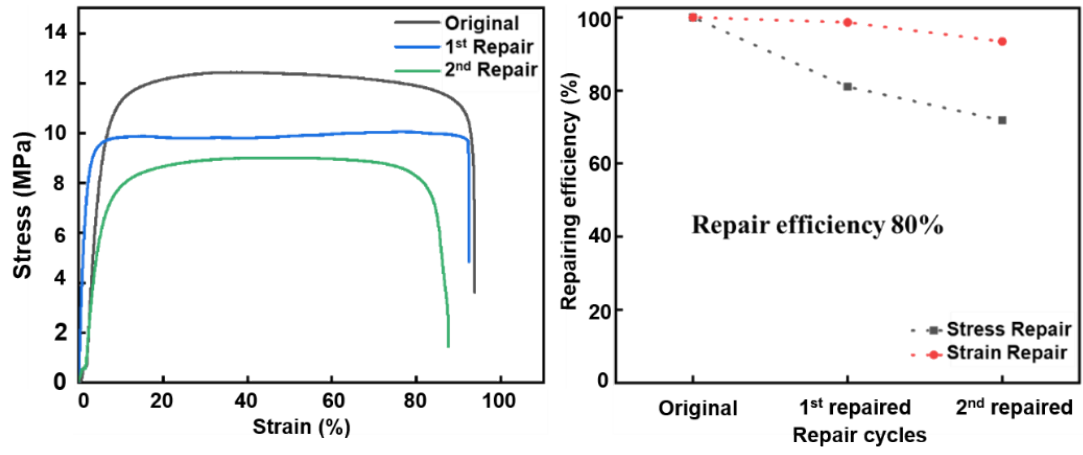


Figure S10. PUSD-2 repair stress–strain diagram and repair efficiency diagram

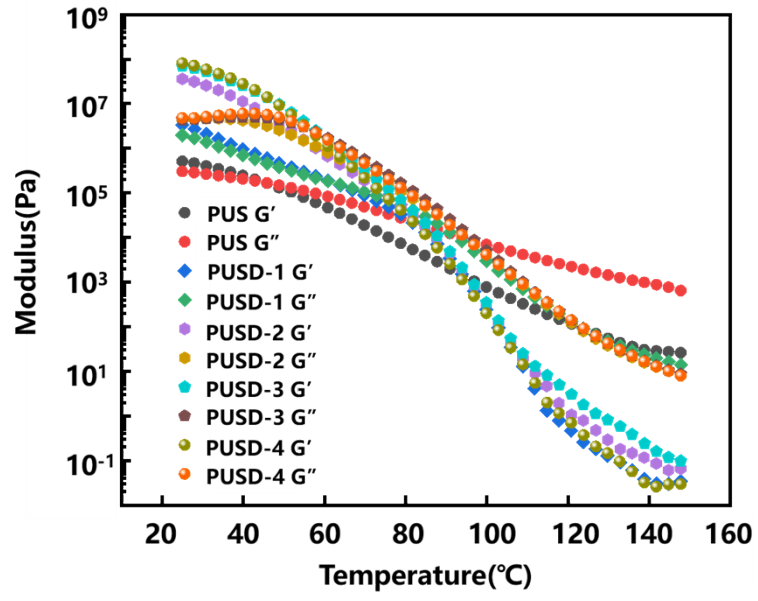


Figure S11. Rheological results of the polymers with different DA contents

Table S3. The moduli of the polymers with different DA contents

Modulus Chart		
Component	Storage modulus (Pa)	Transition temperature (°C)
PUS	5.11×10^5	45.8
PUSD-1	3.32×10^6	62.8
PUSD-2	3.58×10^7	55.8
PUSD-3	6.98×10^7	59.8
PUSD-4	8.15×10^7	56.8

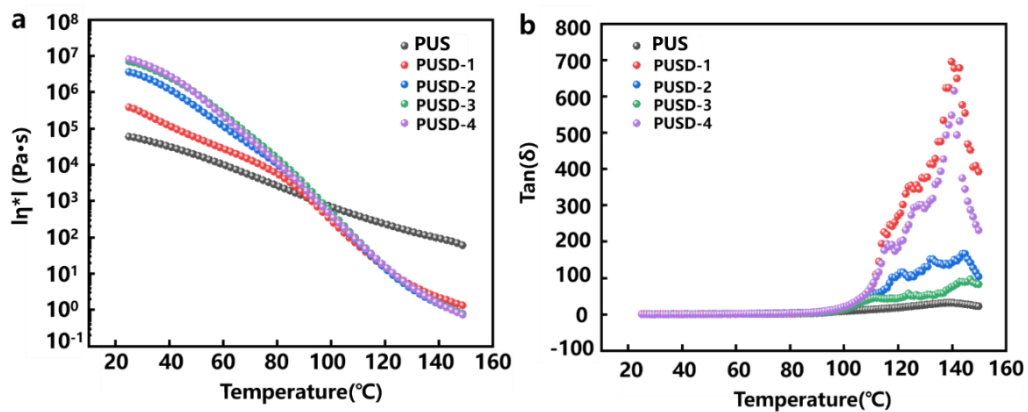


Figure S12. Viscosities and $\tan \delta$ of the polymers with different DA contents

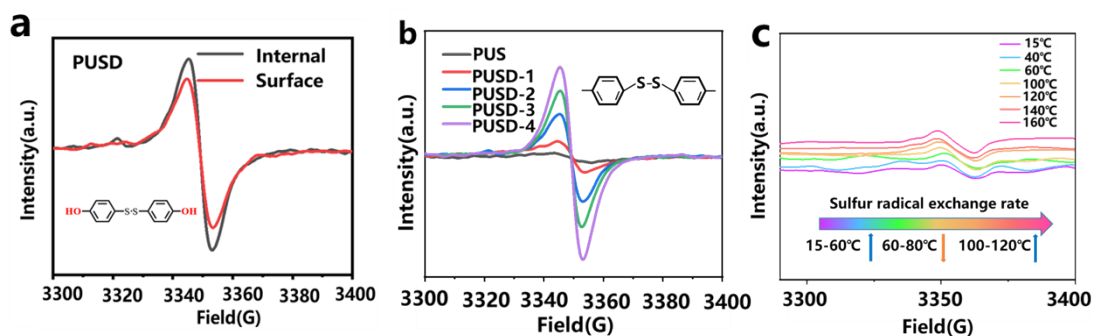
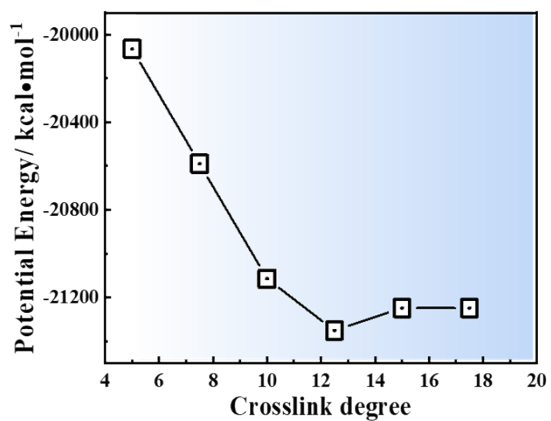


Figure S13. Graphs of the electronic resonance curves of the polymers: a. The electron resonance diagrams of PUSD under different chemical states; b. Electronic resonance diagrams of the PUSD at different temperatures; c. The electronic resonance images of the polymers with different DA contents.

The sulfur radicals trapping tests were carried out to further confirm the reason for the self-repairing behavior. During the dynamic repair process, the exchange rate of the sulfur radicals in PUSD enhanced owing to the increasing ratio of the DA molecules.

Non-DA structure



DA structure

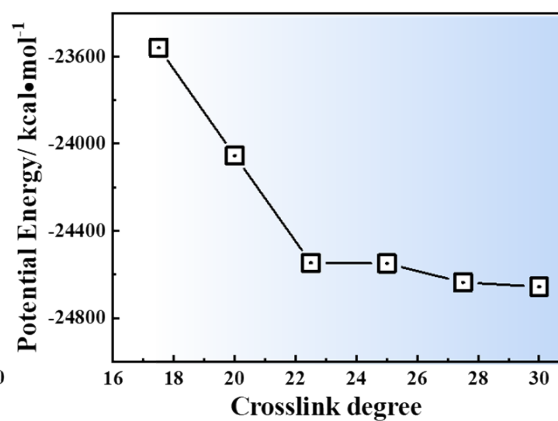


Figure S14. Simulated potential energies versus the crosslinking degree of the PUS (left image) and PUSD (right image) samples

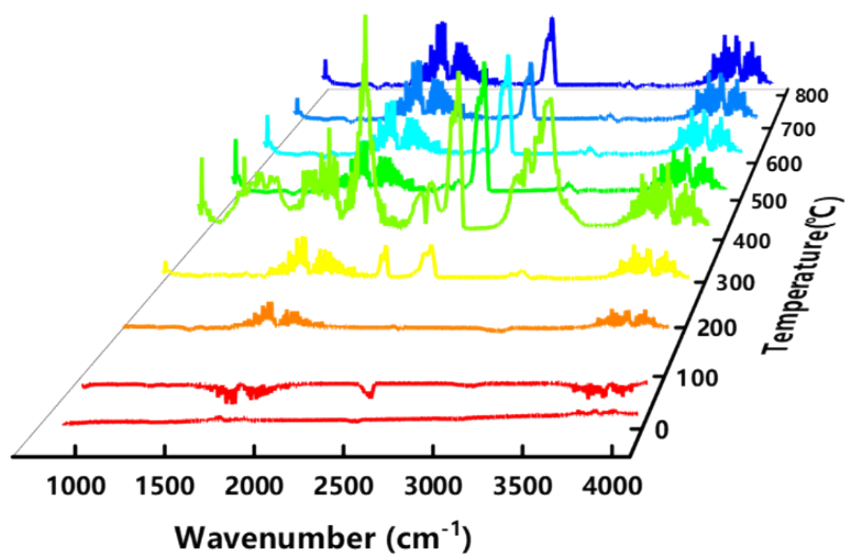


Figure S15. Thermogravimetric and infrared images of the polymers with different DA contents

A fugitive gas collection test analysis was carried out, and no harmful gases (SO_2) escaped until the temperature reached 300 °C.

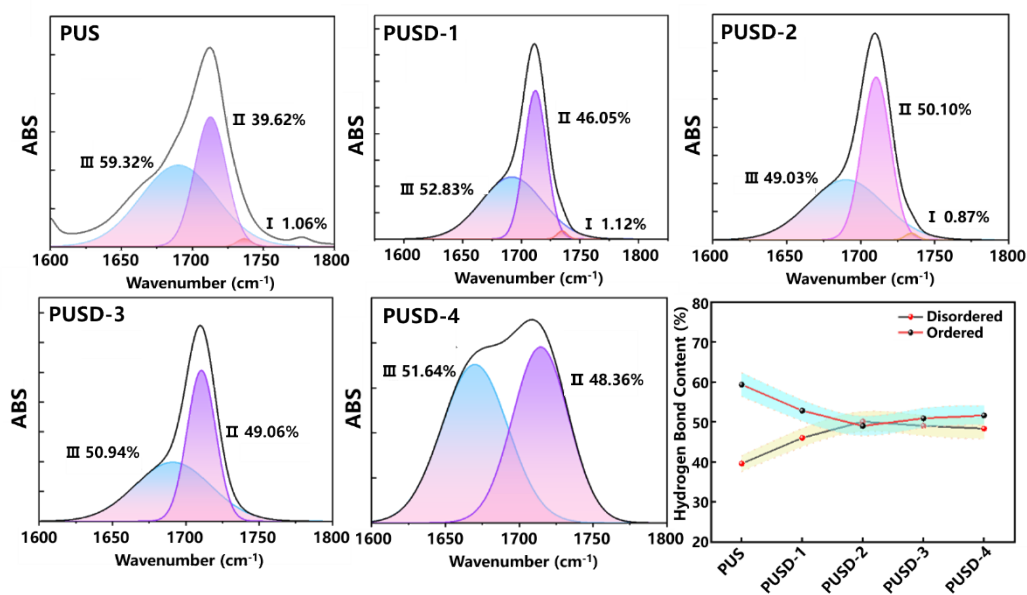


Figure S16. Infrared peaks of the carbonyl bonds of polymers with different DA molecular contents (I: free II: disordered, III: ordered).

In order to repair the large-scale damage of PUSD, the proportion of disordered hydrogen bonds should increase. Therefore, the relative proportions of disordered hydrogen bonds in the PUSD with different DA molecular contents were counted.

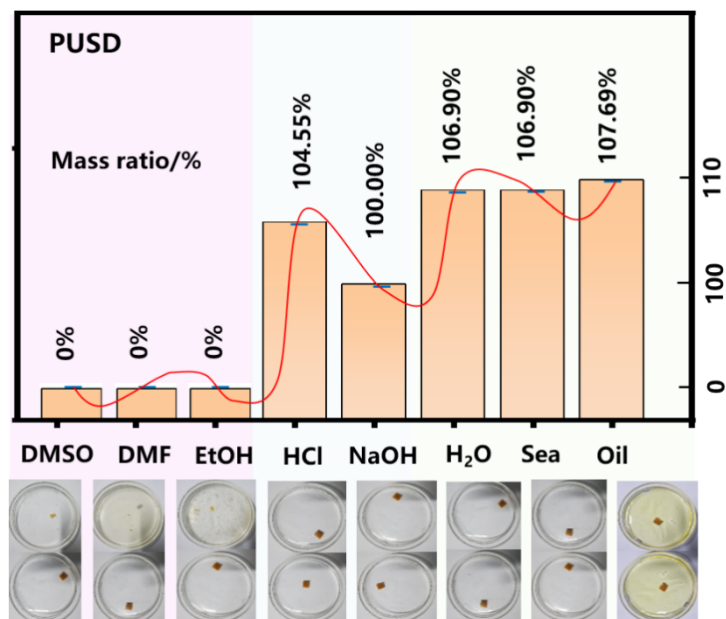


Figure S17. The mass losses of the PUSD immersed in different solvents

In addition to the organic solvent, PUSD can be used in a variety of liquids.

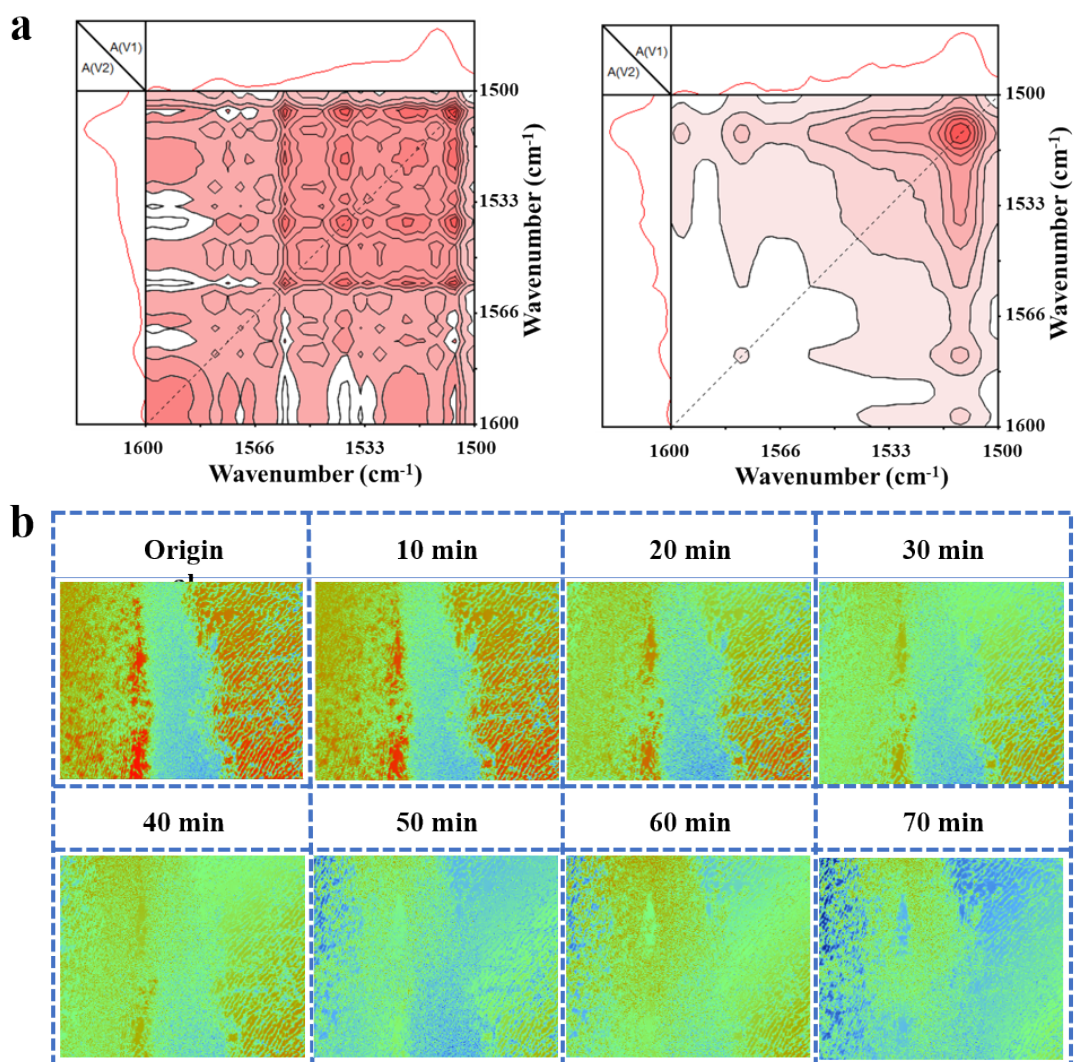


Figure S18. Two-dimensional simultaneous infrared spectrograms and the repairing effect of PUSD at different times.

The dynamic simultaneous and asynchronous IR spectroscopy was performed in the whole repairing process of PUSD. It was found that the carbamate structure was dynamically changing during the repairing process.

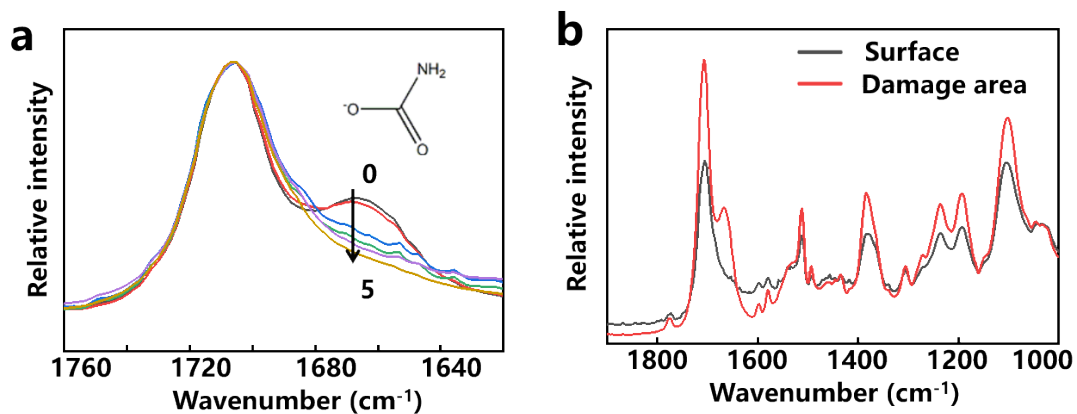


Figure S19. Infrared spectra of the damage area and the undamaged surface of PUSD.

The damage process was investigated with the two-dimensional infrared spectroscopy, and it was found that there was a big difference between the molecular structures of the damage area and the undamaged surface. The undamaged surface of PUSD was rich in soft segments, and the damage area was rich in hard segments. The larger amount of carbamate in the damage region than that on the undamaged surface further demonstrated the difference between the chemical composition on the surface and that in the interior part.

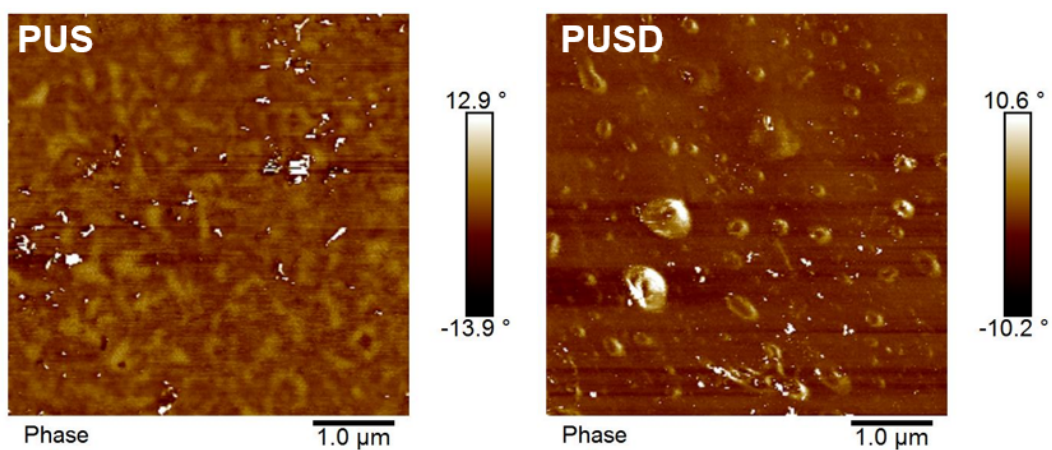


Figure S20. AFM images of PUS and PUSD-2.

As shown in Figure S20, the microphase-separated structure of the self-repairing PUSD systems was further verified by atomic force microscopy, and the results clearly showed the aggregation of both the soft segments (dark areas) and hard segments (bright areas). The PUSD has a distinct microphase separation structure.

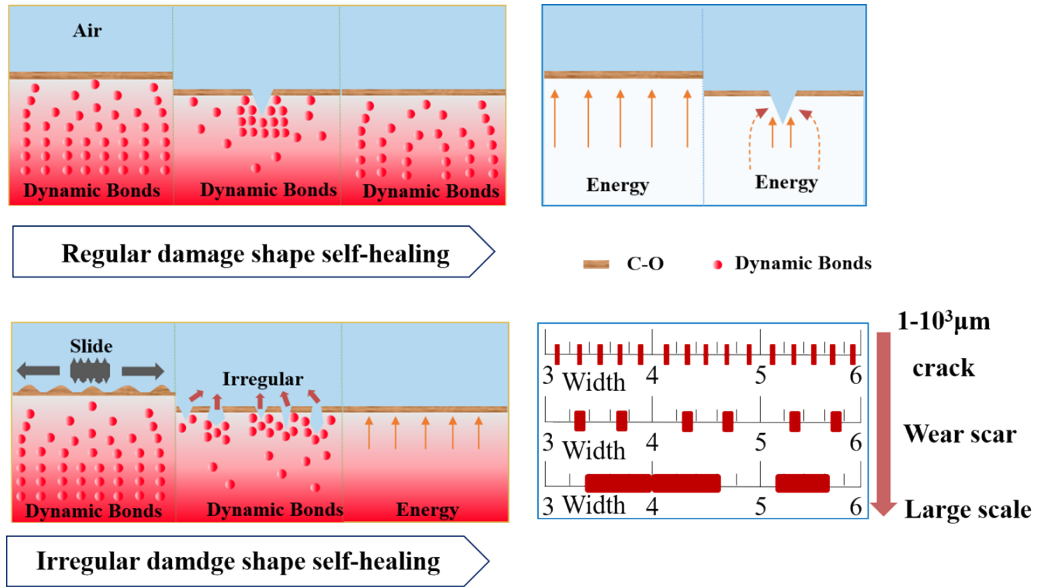


Figure S21. Diagram of the repair mechanism of the PUSD

As shown in Figure S21, this type of polyurethane allows for the targeted repair of damage at different scales.